

# Theoretical study of molecular hydrogen clusters

## Growth models and magic numbers

J.I. Martínez<sup>1</sup>, M. Isla<sup>1</sup>, and J.A. Alonso<sup>1,2,a</sup>

<sup>1</sup> Departamento de Física Teórica, Atómica y Óptica, University of Valladolid, 47001 Valladolid, Spain

<sup>2</sup> Donostia International Physics Center (DIPC), 20018 San Sebastián, Spain

Received 24 July 2006 / Received in final form 20 October 2006

Published online 24 May 2007 – © EDP Sciences, Società Italiana di Fisica, Springer-Verlag 2007

**Abstract.** Hydrogen clusters are formed by packing H<sub>2</sub> molecules. A structural characterization of (H<sub>2</sub>)<sub>N</sub> clusters up to  $N = 35$  has been carried out at zero temperature by using density functional theory. The binding between the hydrogen molecules is very weak and the cluster growth reminds that of the inert gas clusters. An icosahedron is obtained for (H<sub>2</sub>)<sub>13</sub>. For clusters larger than (H<sub>2</sub>)<sub>13</sub> several growth models have been compared. The binding energy indicates specially stable clusters for some particular sizes. The magic numbers can be related to Raman spectroscopy experiments, where the intensity of the Raman signal serves to assign enhanced abundance to clusters with  $N \approx 13, 32, 55$ , which coincide with some of the most stable clusters obtained in the present study. In addition, comparison of theory and experiment suggests that clusters with  $N$  smaller than 27 are liquid. The photoabsorption spectra have been calculated using time-dependent density functional theory. Those spectra can be interpreted as a widening of the absorption peaks of the H<sub>2</sub> molecule due to the various environments experienced by different molecules in the same cluster.

**PACS.** 30. Atomic and molecular physics – 31. Electronic structure of atoms and molecules: theory – 31.15.Ew Density-functional theory

## 1 Introduction

Hydrogen clusters have attracted attention due to their peculiar properties [1] that arise from the coexistence of strong intramolecular bonding and weak intermolecular forces. Most investigations have focussed on clusters of the family H<sub>3</sub><sup>+</sup>(H<sub>2</sub>)<sub>n</sub> with  $n = 1, 2, \dots$  with the result that their structure, energetics and response to intense laser pulses are nowadays well-known [2,3]. Their easiness to be handled experimentally [4], and the fact that the majority of the hydrogen clusters in the universe belong to this family, justify the study of the ionized species. In contrast, there are few studies of neutral clusters [5–8]. Those works suggest the formation of shells of molecules, and the first experimental evidence has been provided by Raman spectroscopy experiments performed in cryogenic jets of the pure gas [7]. Those experiments have been interpreted as indicating the formation of complete shells for certain *magic numbers*,  $N \approx 13, 32$  and 55. Nevertheless, a model to explain the formation of the closed shell structures does not exist. The main purpose of this work is to study the atomic structure of neutral hydrogen clusters by performing Density Functional (DFT) calculations. We find that the H<sub>2</sub> molecule behaves as a rather spherical unit and

that the growth of the (H<sub>2</sub>)<sub>N</sub> clusters has some similarities with the well-known growth of the inert gas clusters [1].

## 2 Structure and growth

For the calculation of the ground-state electronic configurations, we have used an implementation of DFT in which the Kohn-Sham equations are solved using a supercell geometry and a basis of plane waves to expand the wavefunctions. For numerical purposes the electron-proton interaction is modelled by an effective potential [9]: a pseudopotential for hydrogen has been generated following the scheme of Troullier and Martins [10]. We have used a cubic supercell of size  $30 \times 30 \times 30$  a.u.<sup>3</sup> and a single  $k$  point. The basis of plane waves has an energy cutoff of 50 Rydberg. Due to the weak intermolecular interactions in these clusters, the supercell size and the cutoff have been adjusted in order to achieve sufficient accuracy in the total energy. Previous work [11] involving the interaction between hydrogen molecules adsorbed on carbon nanotubes gave reasonable results using the local density approximation (LDA) for exchange and correlation. For this reason an LDA parametrization of Perdew and Wang [12] is adopted here. Test calculations using the

<sup>a</sup> e-mail: jaalonso@fta.uva.es

generalized gradient approximation (GGA) gave unsatisfactory results. Effects of the nuclear spin have not been considered.

For the optimization of the structures we took initial geometries with the atoms placed at random positions. Starting from those geometries we have performed structural relaxations using a steepest-descent algorithm and a convergence criterion of  $10^{-5}$  Hartree/a.u. for the force on every atom. Formation of molecules occurs in all cases, revealing the molecular character of the clusters. A molecular bond length of 1.38 a.u., close to the experimental value of 1.40 a.u. for the isolated  $H_2$  molecule [13], is obtained, independent of the cluster size. For  $(H_2)_N$  clusters up to  $N = 13$ , hundreds of geometries have been optimized. In the optimized structure of  $(H_2)_2$  the two molecules are in a perpendicular configuration, a triangle is obtained for  $N = 3$ , and a bent rhombus for  $N = 4$ . The structures obtained belong to the  $D_{3h}$  symmetry group for  $N = 5$  (triangular bipyramid), to  $O_h$  for  $N = 6$  (square bipyramid), and to  $D_{5h}$  for  $N = 7$  (pentagonal bipyramid). The optimized structures agree in most cases, but not in all, with those obtained by Moller-Plesset (MP2) and Coupled Cluster (CC) methods [6]. The CC calculations predict for  $(H_2)_2$  a different perpendicular configuration, a T-shape. The prediction for  $(H_2)_5$  is a single pyramid, although this structure was obtained using a model potential with parameters fitted to the potential energy surface of smaller clusters. Returning to the DFT results, larger clusters follow a pattern of icosahedral growth and a complete icosahedron is obtained for  $N = 13$ . In this cluster, one molecule occupies the central position and the other 12 molecules occupy the 12 vertices of the icosahedron. A decahedral growth model was also tested for this small-size range, but it led to structures higher in energy. The growth pattern obtained is the same one followed by clusters of the inert gases [1]. The explanation for this behavior is that the hydrogen molecule has a filled electronic shell and, consequently, the intermolecular bonding is very weak. Although the molecules are not perfectly spherical, the hard core character of the short-distance part of the intermolecular potential leads to structures similar to those of inert gas clusters.

The above results and the results of a recent experimental work [7], in which Raman spectroscopy revealed the existence of some magic numbers, have motivated us to restrict the study of the structures of larger clusters to several growth models based on the decoration of the icosahedron. An icosahedron is formed by 20 triangular faces joined by 30 edges and 12 vertices. Additional molecules can be added on top of the icosahedral core in different ways. In a first type of covering, molecules are added on top of edge (E) and vertex (V) positions. These provide a total of 42 sites ( $30 + 12$ ) to cover  $(H_2)_{13}$ , and a cluster with 55 molecules is obtained after full covering. This is called multilayer icosahedral (MIC) growth. Alternatively, one can cover V sites and the 20 F sites at the center of the triangular faces. In this way, the covering of  $(H_2)_{13}$  by 32 additional molecules ( $12 + 20$ ) leads to a cluster with 45 molecules. This second type of covering is often

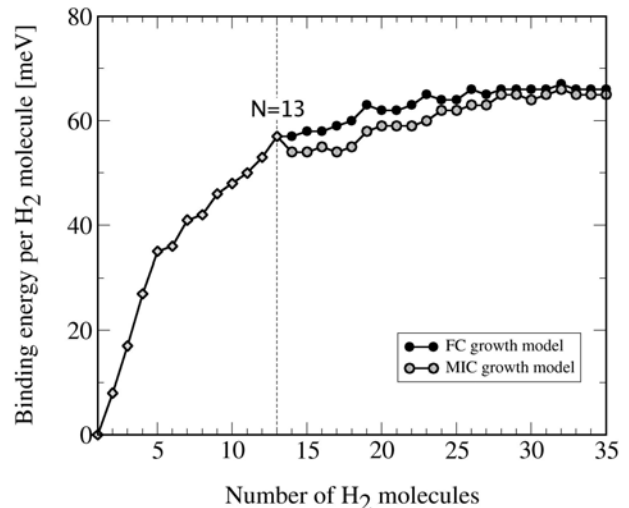


**Fig. 1.** Binding energy per molecule for the most favorable growth paths (FC and MIC growth models), up to  $N = 35$ .

called face centered (FC) growth. Other growth models, such as the formation of face centered cubic (fcc) cuboctahedral structures, also studied here up to  $N = 33$ , lead to structures of much higher energies.

The optimization of the FC and MIC structures up to  $N = 35$  (of course, the molecules are allowed to optimize their relative orientations) produces the trends shown in Figure 1, where we have plotted the binding energy per  $H_2$  molecule,  $e_b(N)$ ,

$$e_b(N) = \frac{E_b(N)}{N} = \frac{E((H_2)_N) - NE(H_2)}{N} \quad (1)$$

calculated from the ground state energies of the clusters and the free molecule. The FC structures are more stable than the MIC structures at least up to  $N = 35$ . FC growth is also characteristic of the inert gas clusters, but a transition to MIC structures [1] occurs at  $N = 27-28$ . Here, the transition has not yet occurred at  $N = 35$ . Nevertheless, the difference between the binding energies of the FC and MIC structures decreases as  $N$  increases, and at  $N = 35$  the two structures are practically degenerate, so a transition to MIC structures is expected soon. The fact that  $H_2$  molecules are not spheres appears to be responsible for the increased stability range of the FC structures. Two examples of FC structures, the ground states of  $(H_2)_{19}$  and  $(H_2)_{23}$ , are shown in Figure 2. The first one is obtained by decorating the icosahedron with a six-molecules umbrella (the light color molecules in the figure). Addition of an adjacent umbrella leads to the structure of  $(H_2)_{23}$ . Local maxima of the binding energy per molecule are obtained in Figure 1 for these two clusters. Other local maxima, for  $N = 26$  and  $32$ , correspond to filling additional umbrellas. The distance between neighbor molecules has an average value of 5.4 a.u., almost independent of the cluster size.

The binding energies of Figure 1 have been obtained with the LDA and, furthermore, do not contain zero point corrections. The LDA is known to overestimate binding energies. This fact compensates for the neglect of

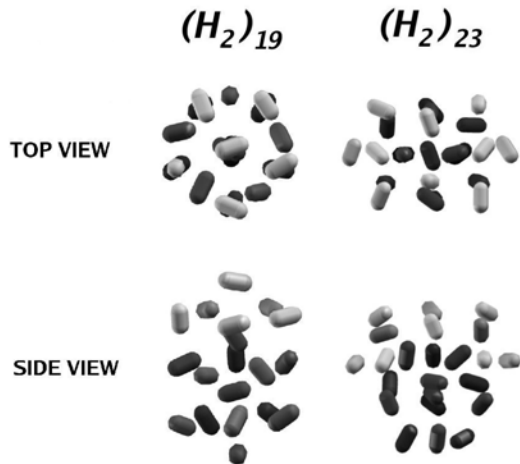


**Fig. 2.** Ground state structure of  $(\text{H}_2)_{19}$  and  $(\text{H}_2)_{23}$ . These configurations arise by capping the icosahedral core (dark molecules) with one umbrella (light  $\text{H}_2$  molecules) and with two adjacent umbrellas, respectively.

van der Waals interactions, but still overestimates  $e_b$ . A total binding energy  $E_b$  between 4 and 5 meV is obtained for  $(\text{H}_2)_2$  in the MP2 and CC methods [6, 14], and the LDA gives 15 meV (twice the value of  $e_b$  in Fig. 1). Considering the tiny binding energy, this is quite successful for DFT, and it is probably the most one can expect from a simple density functional. Because all clusters are subject to similar errors, trends in the binding energy as a function of  $N$  are more trustable. Zero point vibrational corrections reduce substantially the binding energy. We have calculated the zero point vibration for  $(\text{H}_2)_2$ . The intermolecular potential is very anharmonic. Accounting for anharmonicity effects in first order [15], a corrected value of 2.2 meV is obtained for the total binding energy  $E_b$ . Similar reductions affect other clusters. These small binding energies have important consequences, as we discuss below. Zero point binding energies are also reduced substantially in the ab initio calculations [6].

Figure 3 shows the relative stability of the clusters, defined by the expression

$$\Delta e_b(N) = 2e_b(N) - [e_b(N+1) + e_b(N-1)] \quad (2)$$

where  $e_b(N)$  is the binding energy per molecule, for the FC and MIC structures. The peaks in  $\Delta e_b(N)$  at  $N = 5, 7, 13, 19, 23, 26$  and  $32$  for FC structures can also be seen in Figure 1 as peaks ( $N = 13, 19, 23, 26, 32$ ) or changes of slope ( $N = 5, 7$ ). The peaks for  $N$  larger than 13 correspond to the progressive formation of umbrellas. These findings are consistent in part with the results of a recent experiment [7] in which the Raman intensity was measured in cryogenic jets of hydrogen clusters. Local maxima in the Raman intensity were observed for  $N \approx 13, 32$  and  $55$ , and were ascribed to a larger abundance of those clusters. The present theoretical analysis provides an interpretation of the first two magic sizes. In addition, the trend in the FC and MIC binding energies displayed in Figure 1 suggests that an FC to MIC transition is likely to occur immediately, which would explain the experimen-

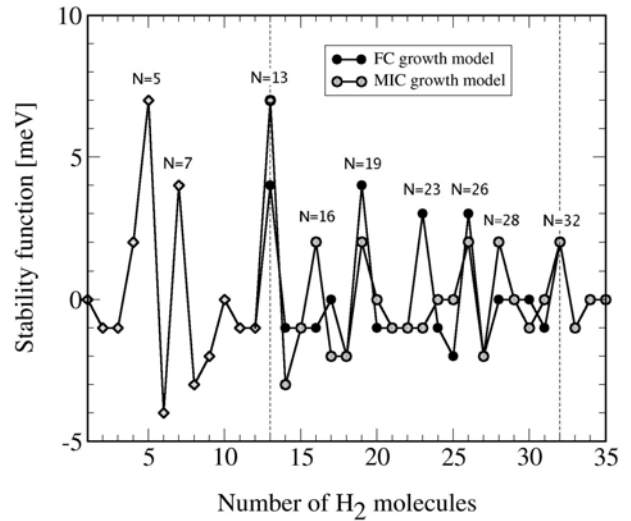


**Fig. 3.** Stability function,  $\Delta e_b(N)$ , of  $(\text{H}_2)_N$  clusters for MIC and FC growth models. Peaks correspond to clusters with enhanced stability. Vertical lines indicate features observed in a Raman spectroscopy experiment.

tal magic cluster  $(\text{H}_2)_{55}$  as a MIC icosahedron with two complete shells. Notice that  $N = 32$  is also a peak in the binding energy of clusters with the MIC structure (see Figs. 1 and 3).

However, the other peaks in Figures 1 and 3 have not been detected in the Raman experiments. Our calculations correspond to solid-like clusters with a well defined structure. But, as indicated above, zero point energies reduce so much the binding energies that it is likely that many of these clusters are liquid even at very low temperatures. This is supported by the tiny difference in binding energy between FC and MIC isomers, and is confirmed by path integral Monte Carlo simulations [8]. These simulations, which use model intermolecular potentials, have predicted that most  $(\text{H}_2)_N$  clusters with  $N$  smaller than 27 are liquid. Thus, effects due to particularly stable solid-like structures can only be observed for clusters larger than  $N = 27-28$ . This explains why  $(\text{H}_2)_{32}$  and  $(\text{H}_2)_{55}$  are the only solid clusters detected in the Raman experiments. Further confirmation comes from the fact that clear magic peaks are seen in the experiments only at the lowest temperatures studied. The case  $N = 13$  is special. Packing arguments suggest that a structure of a central molecule surrounded by a closed shell of 12 molecules is expected even if the cluster is liquid; in this case the surface shell is melted.

### 3 Photoabsorption spectrum

Nuclear fusion between deuterium nuclei has been observed in experiments in which a beam of large deuterium clusters is irradiated by an intense femtosecond laser [16]. These and other experiments involving the laser irradiation of hydrogen clusters provide motivation to calculate the photoabsorption spectrum. This has been obtained

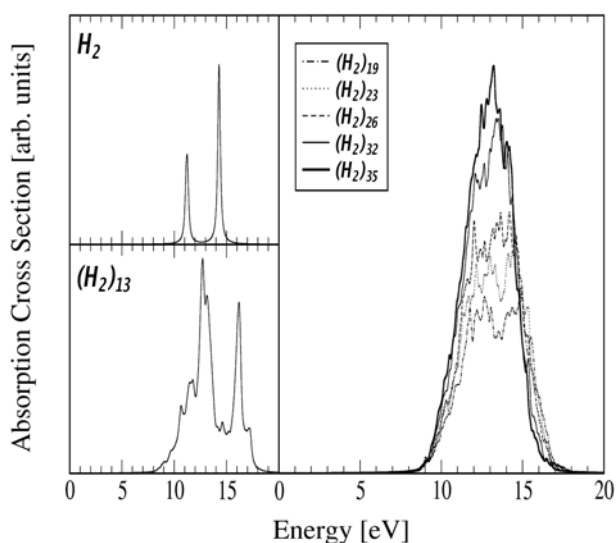


**Fig. 4.** Photoabsorption cross sections for  $(\text{H}_2)_N$  clusters with  $N = 1, 13, 19, 23, 26, 32$  and  $35$ . The absorption strength (in arbitrary units) is scaled in each case in order to obtain a better visualization.

using the time-dependent DFT [17], employing the formalism developed by Casida [18], as implemented in the OCTOPUS code [19]. The finite width of the peaks in an experimental spectrum — linked to the accessible resolution — is mostly determined by the temperature. In our calculations each peak in the spectrum has been broadened by a Lorentzian profile of width equal to 0.005 a.u., which is a value commonly used to mimic the experimental resolution. The adiabatic LDA description of exchange and correlation has been used successfully in the calculation of the photoabsorption spectrum of atoms and atomic clusters [20–22], although no experience exists for hydrogen clusters. Figure 4 shows the photoabsorption cross sections for several clusters. No absorption occurs for energies below about 9 eV, due to the large gaps between the highest occupied and the lowest unoccupied molecular orbitals. The spectrum of the hydrogen molecule shows peaks at 11.2 eV and 14.3 eV. The structure of two peaks is preserved as the cluster grows up, but the peaks are widened and slightly shifted to higher energies. This indicates that the spectrum of the clusters is based on the individual contributions of the hydrogen molecules. The changes show the influence of the weak intermolecular interactions, and the increased width of the peaks is a consequence of different molecules experiencing different environments in the same cluster. Due to the same effect, the two peaks progressively merge into a single wide peak for sufficiently large clusters. We conclude that the evolution of the photoabsorption spectrum of  $(\text{H}_2)_N$  clusters is consistent with the molecular character of the clusters.

Work was supported by MEC of Spain (Grant MAT2005-06544-C03-01), and by Junta de Castilla y León (Grant VA039A05). J.I.M. and M.I. acknowledge support from MEC under the FPI and FPU graduate fellowship programs, respectively.

## References

1. J.A. Alonso, *Structure and Properties of Atomic Clusters* (Imperial College Press, London, 2005), see Chap. 3
2. M. Isla, J.A. Alonso, *Phys. Rev. A* **72**, 023201 (2005)
3. M. Ma, P.G. Reinhard, E. Suraud, *Eur. Phys. J. D* **33**, 49 (2005)
4. B. Farizon, M. Farizon, M.J. Gaillard, F. Gobet, M. Carré, J.P. Buchet, P. Scheier, T.D. Märk, *Phys. Rev. Lett.* **81**, 4108 (1998)
5. M.V. Rama Krishna, K.B. Whaley, *Z. Phys. D* **20**, 223 (1991)
6. M. Carmichael, K. Chenoweth, C.E. Dykstra, *J. Phys. Chem. A* **108**, 3143 (2004)
7. G. Tejada, J.M. Fernández, S. Montero, D. Blume, J.P. Toennies, *Phys. Rev. Lett.* **92**, 223401 (2004)
8. F. Mezzacapo, M. Boninsegni, *Phys. Rev. Lett.* **97**, 045301 (2006)
9. M. Ma, P.G. Reinhard, E. Suraud, *Eur. Phys. J. D* **14**, 217 (2001)
10. N. Troullier, J.L. Martins, *Phys. Rev. B* **43**, 1993 (1991)
11. I. Cabria, M.J. López, J.A. Alonso, *Comput. Mater. Sci.* **35**, 238 (2006)
12. J.P. Perdew, Y. Wang, *Phys. Rev. B* **45**, 13244 (1992)
13. N.A. Lange, G.M. Forker, *CRC Handbook of Physical Chemistry* (McGraw-Hill, New York, 1969)
14. P. Diep, J.K. Johnson, *J. Chem. Phys.* **112**, 4465 (2000)
15. B.H. Bransden, C.J. Joachain, *Physics of Atoms and Molecules* (Longman, Essex, 1999), p. 391
16. T. Ditmire, J. Zweiback, V.P. Yanovsky, T.E. Cowan, G. Hays, K.B. Wharton, *Nature* **398**, 489 (1999)
17. E.K.U. Gross, J.F. Dobson, M. Petersilka, in *Topics in Current Chemistry*, edited by R.F. Nalewajski (Springer Verlag, Heidelberg, 1996), Vol. 81, p. 81
18. M.E. Casida, in *Recent Advances in Density Functional Methods*, edited by D.P. Chong (World Scientific, Singapore, 1995), Part I, p. 155
19. M.A.L. Marques, A. Castro, G.F. Bertsch, A. Rubio, *Comput. Phys. Commun.* **151**, 60 (2003)
20. A. Rubio, J.A. Alonso, X. Blase, L.C. Balbás, S.G. Louie, *Phys. Rev. Lett.* **77**, 247 (1996)
21. A. Castro, M.A.L. Marques, J.A. Alonso, G.F. Bertsch, K. Yabana, A. Rubio, *J. Chem. Phys.* **116**, 1930 (2002)
22. J.I. Martínez, A. Castro, A. Rubio, J.M. Poblet, J.A. Alonso, *Chem. Phys. Lett.* **398**, 292 (2004)